DOI: 10.21062/mft.2025.062 http://www.journalmt.com

Fast and Cost-effective Calibration Method of Assembly Errors on Rotary Axes of Five-axis Machine Tools

Yongqiang Pan (0009-0004-4242-1177), Yue Tang (0009-0004-0331-9065)*
Aviation Equipment Manufacturing Industry College, Chengdu Aeronautic Polytechnic University, Chengdu, 610100, China. *E-mail: tangyue_2020@163.com

Five-axis machine tools are key equipment to process impellers, blades, and other precision mechanical parts. However, the accuracy of the machine tools is significantly influenced by assembly errors, and over time, these errors may change, further impacting the machining accuracy. Traditional laser interferometry technology can identify such assembly errors. The development of on-machine measurement technology has enabled methods that utilize on-machine measurement for assembly error calibration, improving calibration efficiency. The study introduces an efficient method to calibrate the assembly errors of machine tool rotary axes. First, the kinematic model for a machine tool is develop. Subsequently, utilizing on-machine measurement technology, the assembly errors of the rotary axes are calibrated, and the calibration uncertainty is analyzed. The results of the experiment confirm the validity of the calibration method. This method can be applied for periodic calibration of machine tool assembly errors, continuous monitoring variations in machine tool accuracy and ensuring the stability of machining quality.

Keywords: Assembly errors, Calibration, Machine tools, On-machine measurement

1 Introduction

Five-axis machine tools are important equipment to process complex mechanical parts. With the continuous increase in the precision requirements for part processing, it is essential to enhance and sustain the precision of machine tools. [1-3]. The calibration of linear axis assembly errors is relatively mature, but the impact of rotary axis assembly errors on machine tool precision is greater compared to linear axes [4-5].

The ball-bar device is commonly employed for calibrating machine tool assembly errors. During the calibration, two standard balls of the ball-bar are mounted on the magnetic base of the spindle and the table of the machine tool. The calibration is performed by analyzing the relationship between the relative motion trajectory and assembly errors [5-7]. Xiang et al. [8] adopted the ball-bar to track different motion trajectories, ultimately calibrated eight machine tool assembly errors. In order to calibrate the assembly errors, the ball-bar requires multiple adjustments of the installation position to accommodate different motion trajectories. This multi-step installation process is labor-intensive, and it may also lead to setup errors in the ball-bar itself. The R-test, consisting of three high-precision linear displacement sensors, is usually applied to indirectly calibrate assembly errors on rotary axes. Compared to the double ball-bar, the R-test does not require multiple trajectories to resolve the motion components of each axis, improving the calibration efficiency of assembly errors [9-10]. However, the R-test equipment also requires installation and calibration, and the calibration model for assembly errors is more complex [11]. Laser tracking measurement technology is also used in the calibration of machine tool assembly errors. By applying multi-station time-sharing measurement technology of the laser tracker, the relationship between the measurement trajectory and station positions is established, enabling assembly error calibration. Deng et al. [12] considered rigid body constraints and used the laser tracker to calibrate eight machine tool assembly errors. However, the laser tracker is bulky, difficult to integrate into machine tools, and prone to loss of signal, which affects calibration efficiency [13-14].

In addition, many researchers have attempted to use machine tool cutting standard workpieces to calibrate machine tool assembly errors. This method first designs a specific shape of a workpiece and then uses the machine tool to cut this standard workpiece. By comparing the theoretical model and the actual processed part, assembly errors can be calibrated [15]. Yang et al. [16] used the cutting of shaft-type parts to calibrate eight rotary axis assembly errors. However, machine tool cutting is a complex process, easily influenced by other factors such as thermal effects, cutting force, and machine tool vibration, making it difficult to isolate assembly errors [17]. Generally, machine tools process standard workpieces to detect machining

performance, rather than calibrating assembly errors.

For machine tools, periodic calibration of assembly errors can maintain the machining accuracy. According to ISO 230-2, periodic accuracy verification of machine tools is key to maintaining machine tool accuracy. Similarly, ISO 10360-1 emphasizes the importance of intermediate accuracy checks for machine tools. Since periodic accuracy verification is very frequent, the efficiency of calibration is crucial. In recent years, the advancement of on-machine measurement technology has enabled methods that utilize on-machine measurement for assembly error calibration. Compared with other assembly error calibration methods, the on-machine measurement calibration method does not require expensive measuring equipment or specialized operational skills. Moreover, the on-machine measurement is convenient to be integrated in the machine tool, making it easier to automate the calibration process, making it suitable for periodic accuracy calibration of machine tools.

This study introduces a rapid calibration method for machine tool rotary axis assembly errors based on on-machine measurement technology. First, a kinematic model for a machine tool is develop, and assembly errors are defined. Subsequently, utilizing on-machine measurement technology, a rapid calibration model for assembly errors is developed, and the uncertainty of the calibration is calculated. Finally, calibration experiments are performed to validate the correctness of the calibration method.

2 Definition of rotary axis assembly error and kinematic error modeling

Fig. 1 shows a dual-rotary-table five-axis machine tool, consisting of two rotary axes and three linear axes. Coordinate systems are established for each axis. The coordinate systems for the linear axes include the coordinate systems that attaching to X, Y, and Z-axis. These coordinate systems are XCS (X-axis coordinate system), YCS, and ZCS respectively. The coordinate systems of rotary axes are BCS (B-axis coordinate system) and CCS. Additionally, the MCS is defined as machine coordinate system which is attached to the frame of the machine.

During machine tool assembly, the B-axis is first installed on the frame of the machine tool, resulting in linear errors in two directions, δ_{xoB} and δ_{zoB}, as well as angular errors around two directions, ε_{xoB} and ε_{zoB}. Then, the C-axis is installed on the B-axis, and correspondingly, relative to the B-axis, the C-axis also generates linear errors in two directions, δ_{xoC} and δ_{yoC}, as well as angular errors around two directions, ε_{xoC} and ε_{yoC}, as shown in Fig. 2.

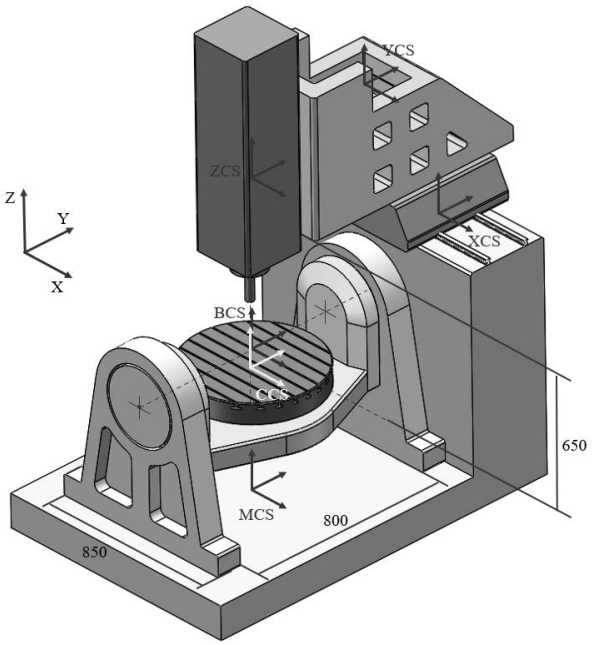

Fig. 1 *Configuration of the dual-rotary-table five-axis machine tool*

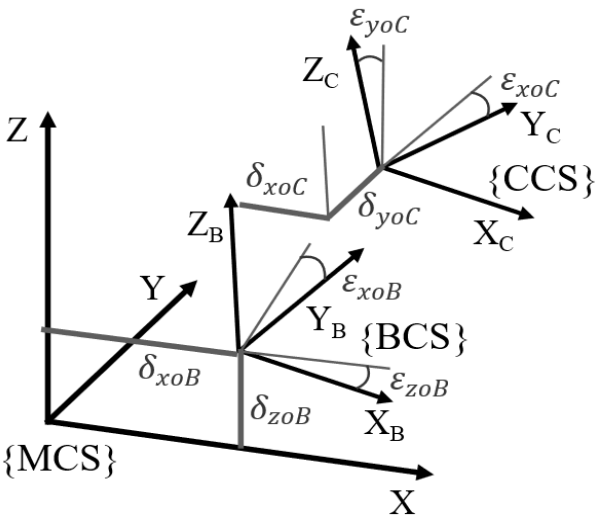

Fig. 2 *Assembly errors of rotary axes*

According to the motion relationships of the components of the five-axis machine tool and the established coordinate systems, the motion transformation relationship from the tool tip to the worktable are described as:

$$ {}^{C}_{Z}T = {}^{C}_{B}T \cdot {}^{B}_{M}T \cdot {}^{M}_{X}T \cdot {}^{X}_{Y}T \cdot {}^{Y}_{Z}T \quad (1) $$

Where ${}^{C}_{Z}T$ denotes the transformation from the CCS to the ZCS, and the meanings of the other matrix symbols are similar. For the linear axes, the transformation from MCS to the ZCS is as follows:

$$ {}^{M}_{Z}T = {}^{M}_{X}T \cdot {}^{X}_{Y}T \cdot {}^{Y}_{Z}T = tr(X_N) \cdot tr(Y_N) \cdot tr(Z_N) \quad (2) $$

Where $tr(X_N)$ represents the motion in the X-direction according to the motion code X_N. Further expansion gives:

$$ {}^{M}_{Z}T = \begin{bmatrix} 1 & 0 & 0 & X_{NC} \\ 0 & 1 & 0 & Y_{NC} \\ 0 & 0 & 1 & Z_{NC} \\ 0 & 0 & 0 & 1 \end{bmatrix} \quad (3) $$

For the rotary axes, due to the presence of assembly errors, the nominal coordinates of the tool tip relative to the worktable will deviate. Thus, the transformation from MCS to CCS can be described as:

$$ {}^{M}_{C}T_e = {}^{M}_{B}T_e \cdot {}^{B}_{C}T_e = E_B \cdot {}^{M}_{B}T \cdot E_C \cdot {}^{B}_{C}T \quad (4) $$

The subscript "e" indicates the transformation matrix including assembly errors, and E_B and E_C represent the error motion matrices caused by the assembly errors of the B-axis and C-axis, respectively. $rot(B_N)$ represents the rotation around the B-axis under the motion instruction (B_N), then:

$$ {}^{M}_{B}T = rot(B_N) = \begin{bmatrix} \cos B_N & 0 & -\sin B_N & 0 \\ 0 & 1 & 0 & 0 \\ \sin B_N & 0 & \cos B_N & 0 \\ 0 & 0 & 0 & 1 \end{bmatrix} \quad (5) $$

Both E_B and E_C contain linear and angular errors. To illustrate the composition of the error motion matrix, we will use the derivation of E_B as an example. First, the linear errors along the X-direction and Z-direction, δ_{xoB} and δ_{zoB}, reflect the small position errors in their respective directions. The resulting error transformation matrices are as follows:

$$ tr(\delta_{xoB}) = \begin{bmatrix} 1 & 0 & 0 & \delta_{xoB} \\ 0 & 1 & 0 & 0 \\ 0 & 0 & 1 & 0 \\ 0 & 0 & 0 & 1 \end{bmatrix} \quad (6) $$

$$ tr(\delta_{zoB}) = \begin{bmatrix} 1 & 0 & 0 & 0 \\ 0 & 1 & 0 & 0 \\ 0 & 0 & 1 & \delta_{zoB} \\ 0 & 0 & 0 & 1 \end{bmatrix} \quad (7) $$

Similarly, the angular error reflects the small angular deviation around the rotary axis. Therefore, the error matrix caused by the angular error are represented as:

$$ rev(\varepsilon_{xoB}) = \begin{bmatrix} 1 & 0 & 0 & 0 \\ 0 & \cos(\varepsilon_{xoB}) & -\sin(\varepsilon_{xoB}) & 0 \\ 0 & \sin(\varepsilon_{xoB}) & \cos(\varepsilon_{xoB}) & 0 \\ 0 & 0 & 0 & 1 \end{bmatrix} \quad (8) $$

Since angular errors are small quantities, equation (8) can be simplified as:

$$ rev(\varepsilon_{xoB}) = \begin{bmatrix} 1 & 0 & 0 & 0 \\ 0 & 0 & -\varepsilon_{xoB} & 0 \\ 0 & \varepsilon_{xoB} & 1 & 0 \\ 0 & 0 & 0 & 1 \end{bmatrix} \quad (9) $$

Similarly, the error transformation caused by ε_{zoB} can be expressed as follows:

$$ rev(\varepsilon_{zoB}) = \begin{bmatrix} 1 & -\varepsilon_{zoB} & 0 & 0 \\ \varepsilon_{zoB} & 1 & 0 & 0 \\ 0 & 0 & 1 & 0 \\ 0 & 0 & 0 & 1 \end{bmatrix} \quad (10) $$

E_B can be obtained by multiplying these error transformation matrices:

$$ E_B = tr(\delta_{xoB}) \cdot tr(\delta_{zoB}) \cdot rev(\varepsilon_{xoB}) \cdot rev(\varepsilon_{zoB}) \quad (11) $$

$$ E_B = \begin{bmatrix} 1 & -\varepsilon_{zoB} & 0 & \delta_{xoB} \\ \varepsilon_{zoB} & 1 & -\varepsilon_{xoB} & 0 \\ 0 & \varepsilon_{xoB} & 1 & \delta_{zoB} \\ 0 & 0 & 0 & 1 \end{bmatrix} \quad (12) $$

Similarly, the result for E_C is given by the following equation:

$$ E_C = \begin{bmatrix} 1 & 0 & \varepsilon_{yoC} & \delta_{xoC} \\ 0 & 1 & -\varepsilon_{xoC} & \delta_{yoC} \\ -\varepsilon_{yoC} & \varepsilon_{xoC} & 1 & 0 \\ 0 & 0 & 0 & 1 \end{bmatrix} \quad (13) $$

3 Calibration model for rotary axis assembly errors

In this section, on-machine measurement is adopted to measure a standard ball to perform fast calibration for the assembly errors on the rotary axes. First, the assembly error of the B-axis is calibrated. A standard ball is fixed on the table, and the C-axis is locked to the zero position. Then, starting from -90° of the B-axis, it is rotated to 90° in 15° intervals. After each rotation, the standard ball is touched using the on-machine measurement probe. Fig. 3 illustrates the rotation and the probing process of the standard ball of the B-axis.

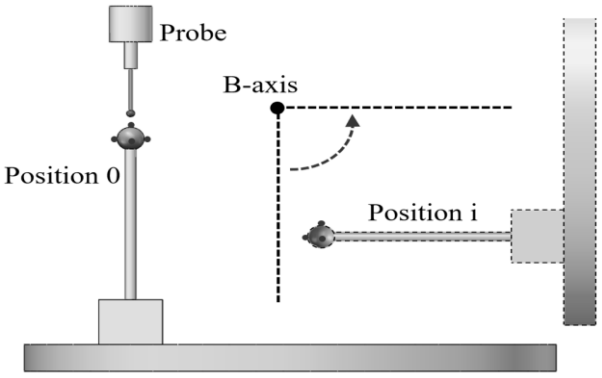

Fig. 3 *Probing process of the standard ball of the B-axis*

When the B-axis is at the zero position, the coordinates of the ball' center in the BCS are denoted as ${}^{B}P_1$. Due to the existence of the assembly errors on B-axis, the transformation from BCS to MCS is as follows:

$$ E_B \cdot {}^{M}_{B}T \cdot {}^{B}P_1 = {}^{M}P_1 \quad (14) $$

Where ${}^{M}P_1$ represents the coordinates of the ball' center in the MCS when the B-axis is at the zero position. Since the B-axis is at zero, the transformation matrix ${}^{M}_{B}T$ is the identity matrix. When the B-axis rotates by an angle B_N, moving from position 0 to position i, as shown in Fig. 3, the coordinate transformation at this point can be expressed as:

$$ E_B \cdot rot(B_N) \cdot {}^{B}P_1 = {}^{M}_{i}P_1 \quad (15) $$

Where ${}^{M}_{i}P_1$ represents the coordinates of the ball' center in the MCS when the B-axis is at the i-th position. By solving equations (14) and (15) together:

$$(E_B)^{-1} \cdot {}^{M}P_1 = rot^{-1}(B_N) \cdot (E_B)^{-1} \cdot {}^{M}_{i}P_1 \quad (16)$$

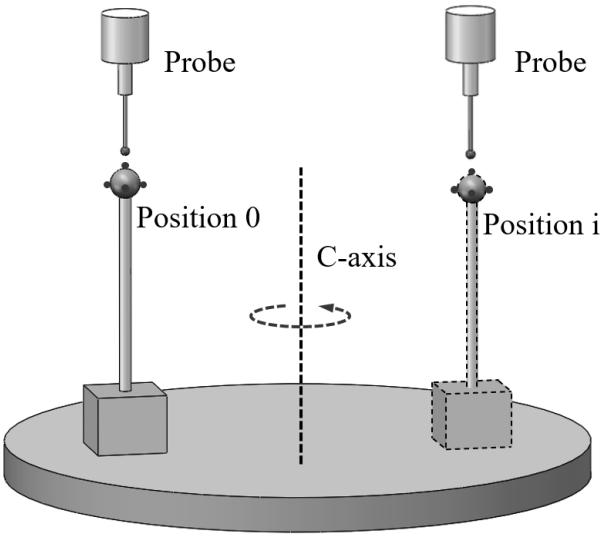

Fig. 4 *Probing process of the standard ball of the C-axis*

The coordinates ${}^{M}P_1$ and ${}^{M}_{i}P_1$ are obtained through on-machine measurement. Since the B-axis assembly error has four components, at least two different angles must be used to obtain the assembly error of the B-axis. Similarly, when measuring the C-axis, the rotation is performed in 30° intervals from -180° to 180°, and at each position, the standard ball is measured using the on-machine measurement, as shown in Fig. 4.

${}^{C}P_2$ represents the coordinates of the ball' center in the CCS when the C-axis is at position 0. From the perspective of machine tool assembly relationships, the C-axis is installed on the B-axis. Unlike the calibration of the assembly errors on B-axis, the coordinates of the center of in the MCS are influenced by both the assembly errors of the B and C-axis. Therefore, the coordinate transformation from CCS to MCS for ${}^{C}P_2$ can be expressed as:

$$E_B \cdot {}^{M}_{B}T \cdot E_C \cdot {}^{B}_{C}T \cdot {}^{C}P_2 = {}^{M}P_2 \quad (17)$$

When the B and C axes are at position 0, the matrices ${}^{M}_{B}T$ and ${}^{B}_{C}T$ are both identity matrices. When the C-axis rotates by the nominal angle C_N, moving from position 0 to position i, the coordinate transformation at this point can be expressed as:

$$E_B \cdot E_C \cdot rot(C_N) \cdot {}^{C}P_2 = {}^{M}_{i}P_2 \quad (18)$$

By solving equations (17) and (18) together, we obtain:

$$(E_C)^{-1} \cdot (E_B)^{-1} \cdot {}^{M}P_2 = rot^{-1}(C_N) \cdot (E_C)^{-1} \cdot (E_B)^{-1} \cdot {}^{M}_{i}P_2 \quad (19)$$

Similarly, the C-axis assembly error matrix also contains four unknowns, requiring at least two rotation positions to solve. It is worthing of noting that the calibration of the assembly errors for the B and C-axis is sequential. The assembly error of the B-axis must be determined first before solving for the assembly error of the C-axis.

4 Calibration experiment verification of assembly errors

The rapid calibration method for rotary axes assembly errors proposed is applied to a dual-rotary-table five-axis machine tool. Configuration of the machine is illustrated in Fig. 1, with additional key parameters provided in Tab. 1. The machine tool is installed with a Renishaw OMP40 probe, which has a ruby ball with a diameter of 6 millimeters at its tip. Before conducting on-machine measurements, the probe system must be calibrated to mitigate the influence of probe system errors on the measurements. This calibration process includes the calibration of probe length, probe offset, and probe pre-travel error, and these calibration steps are executed sequentially according to the macro programs provided by the manufacturer.

Tab. 1 *Key parameters*

X stroke/mm	Y stroke/mm	Z stroke/mm	The diameter of the table/mm	B stroke/deg	C stroke/deg
700	600	500	ϕ630	-65～120	0～360

After calibrating the probe system, a standard ball is placed on the rotary worktable, as shown in Fig. 5. Following the calibration method outlined in Section 3, the standard ball is measured at various rotational angles of the B and C-axis, after which the assembly errors of both axes are calibrated individually. The calibrated assembly errors are summarized in Tab. 2.

According to ISO 10791-6, a ball-bar device is used for circular trajectory testing to validate the correctness of calibration method. This circular trajectory test aims to evaluate the precision of the tool center point trajectory during the rotation of the rotary axis. First, the B-axis is rotated and locked at 10 degrees, followed by the rotation of the C-axis. During the testing process, the ball-bar is installed on the spindle and the table, as shown in Fig. 6. The roundness errors of the circular trajectory before and after compensation are 21.5 μm and 11.6 μm, respectively, as shown in Fig. 7. The verification results shows the effectiveness of the calibration method for rotary axis assembly errors.

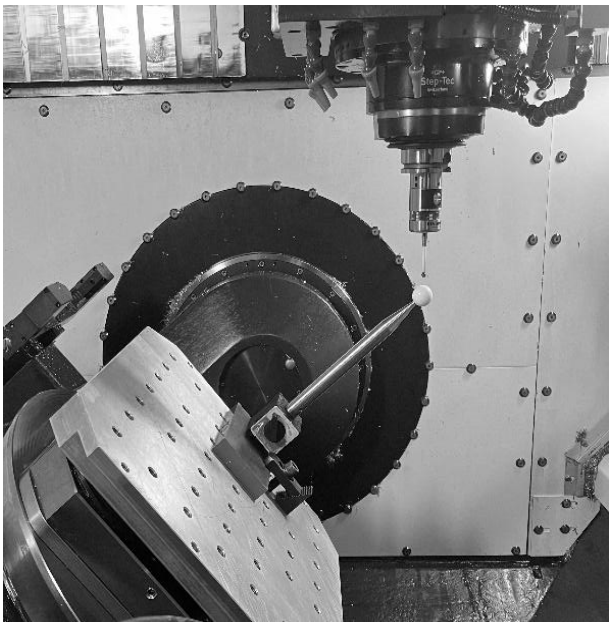

Fig. 5 *Calibration for machine tool rotary axis assembly errors*

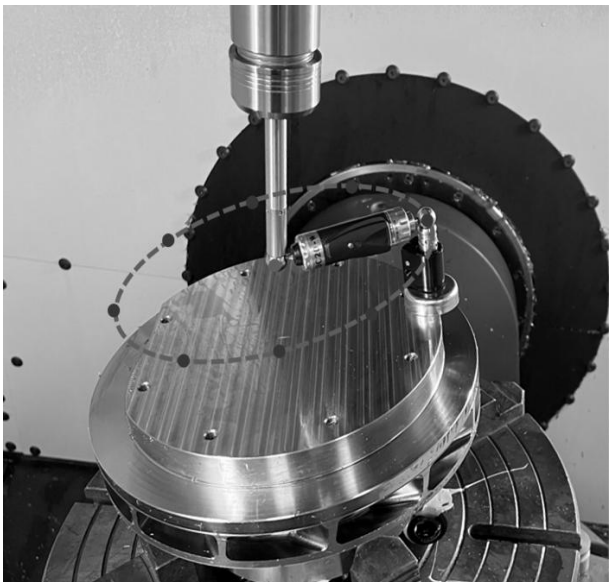

Fig. 6 *Circular trajectory testing*

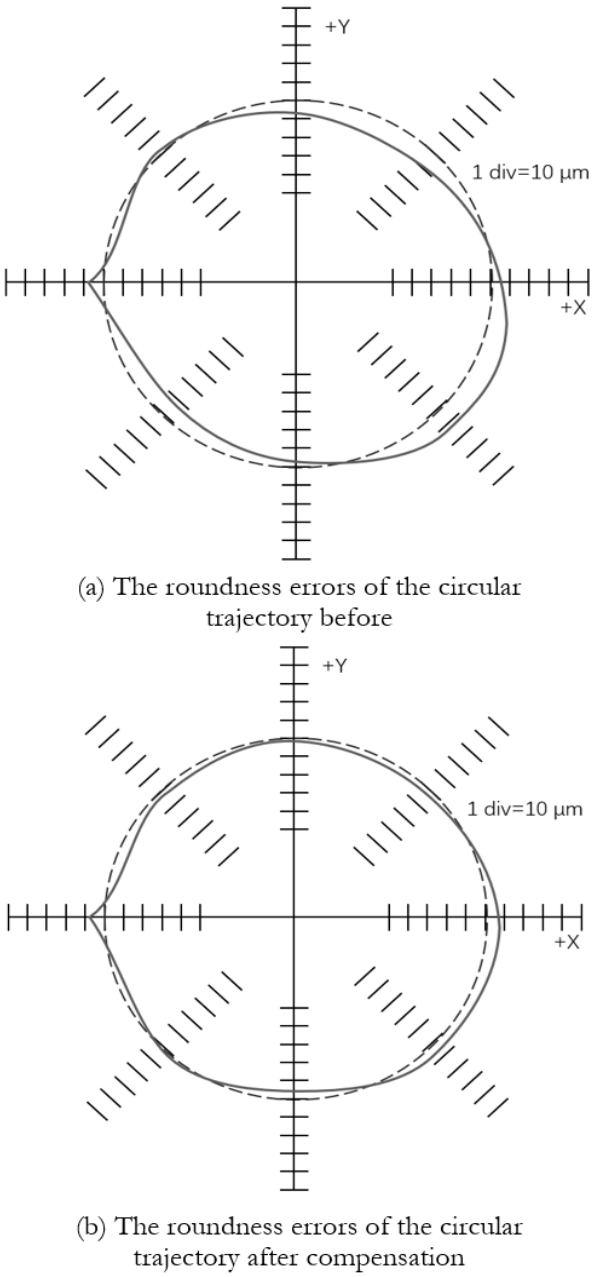

Fig. 7 *The roundness errors of the circular trajectory before and after compensation*

Tab. 2 *Calibrated assembly errors*

	$\boldsymbol{\delta_{xoB}}$/mm	$\boldsymbol{\delta_{zoB}}$/mm	$\boldsymbol{\varepsilon_{xoB}}$/deg	$\boldsymbol{\varepsilon_{zoB}}$/deg
Assembly errors of B-axis	0.0273	-0.0203	-0.00672	0.00285
	$\boldsymbol{\delta_{xoC}}$/mm	$\boldsymbol{\delta_{yoC}}$/mm	$\boldsymbol{\varepsilon_{xoC}}$/deg	$\boldsymbol{\varepsilon_{yoC}}$/deg
Assembly errors of C-axis	- 0.0245	0.0347	-0.00287	- 0.00564

5 Uncertainty analysis of assembly error calibration

The uncertainty of the calibration for the rotary axes assembly errors primarily arises from two aspects. On one hand, it comes from the uncertainty of single-point measurements in on-machine measurement. In addition, the sphericity error of the standard ball also contributes to the calibration uncertainty. This section first employs the Monte Carlo method in conjunction with the error ellipsoid model to analyze the uncertainty brought about by the single-point uncertainty of on-machine measurements.

In on-machine measurement, a contact probe is used to probe the workpiece, and the single-point measurement uncertainty of the probe touching the sample is the main source of measurement error. The single-point measurement uncertainty varies

in different directions when probing the workpiece. If a single sample point is repeatedly probed from different directions, and the random errors in the three directions follow a normal distribution, these points will fill a closed ellipsoidal region, as shown in Fig. 8. The actual size of the ellipsoid will be determined by repeatedly probing the workpiece from three different directions.

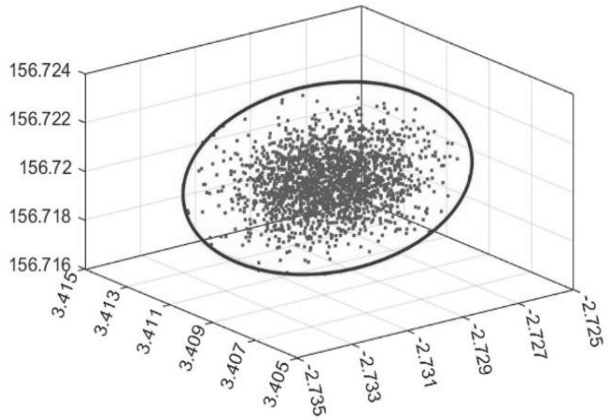

Fig. 8 *Error ellipsoid*

In the rapid calibration experiment of assembly errors, the center of the standard ball is obtained by fitting measurements taken at five points. Based on the single-point measurement uncertainty, five error ellipsoids are generated at these five measurement points on the standard ball. Each time the uncertainty of the assembly error calibration is calculated, a sample point is randomly selected from each error ellipsoid, as shown in Fig. 9. This process may lead to a drift of the standard ball's center, resulting in measurement uncertainty. By repeatedly selecting measurement points from the error ellipsoids, the Monte Carlo method is used to calculate the uncertainty of the error calibration.

In addition, the sphericity error of the standard ball also contributes to the uncertainty in the calibration of assembly errors. Although the manufacturing precision of the standard ball is very high, some sphericity error is inevitably present. Assuming that the sphericity error on the surface of the sphere follows a normal distribution, the Monte Carlo method can also be used to assess the calibration uncertainty caused by the sphericity error. By adding a sphericity error at each point, the center of the ball will also drift, ultimately leading to uncertainty in the calibration of assembly errors. The standard ball used in the experiment has undergone rigorous testing, with a sphericity error of less than 0.5 μm. The calibration uncertainties calculated from the two aspects mentioned above are listed in Tab. 3. The uncertainty results indicate that the uncertainty constitutes a small proportion of the assembly error, demonstrating that the proposed method for calibrating assembly errors is reliable.

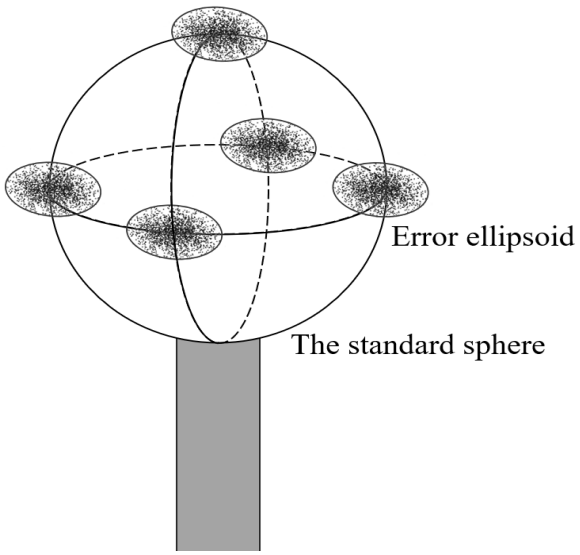

Fig. 9 *Five error ellipsoid around the five points*

Tab. 3 *The uncertainty in the calibration*

	δ_{xoB}	δ_{zoB}	ε_{xoB}	ε_{zoB}
single-point measurement uncertainty	1.7μm	1.6μm	0.00026deg	0.0003deg
sphericity error	0.9μm	0.7μm	0.00008deg	0.00013deg
	δ_{xoC}	δ_{yoC}	ε_{xoC}	ε_{yoC}
single-point measurement uncertainty	1.4μm	2.2μm	0.00023deg	0.00034deg
sphericity error	1.1μm	1.5μm	0.00011deg	0.00025deg

6 Conclusions

With the development of on-machine measurement technology, using on-machine measurement to calibrate machine tool assembly errors can serve as an alternative to traditional assembly error calibration methods. This paper employs the on-machine measurement system of a machine tool to rapidly calibrate the assembly errors of rotary axes of a dual-rotary-table five-axis machine tool. First, the assembly errors are defined, and a kinematic error model is established. The calibration mechanism for the assembly errors

is then described, followed by the application verification of rapid error calibration conducted on the machine tool. Ultimately, all assembly errors on rotary axes of the machine are calibrated, and the effectiveness of the method is validated using the circular trajectory testing. Additionally, an analysis and calculation of the calibration uncertainty are performed, demonstrating the reliability of the proposed assembly error calibration method.

Compared to traditional assembly error methods, the on-machine measurement-based calibration method does not require expensive measuring equipment, such as laser interferometers or laser ball bars, which necessitate specialized operational skills and experience. On-machine measurement systems are being increasingly integrated in machine tools. Allowing for automated calibration processes based on on-machine measurement methods, significantly improving the efficiency of error calibration. Therefore, the on-machine measurement-based calibration method can be used for periodic accuracy checks of machine tool assembly errors, ensuring the stability of machining quality.

Acknowledgement

This research was funded by the Key Natural Science Research Project of Chengdu Aeronautic Polytechnic University in 2024 (ZZX0624087).

References

[1] LI, J., XIE, F., LIU, X. J., et al. (2016). Geometric error identification and compensation of linear axes based on a novel 13-line method. In: *Int J Adv Manuf Technol*, Vol.87, pp. 2269–2283. ISSN 0268-3768

[2] MATU, M., BECHNY, V., JOCH, R. (2024). Identification of Machine Tool Defects Using Laser Interferometer. In: *Manufacturing Technology*, Vol. 24, No. 3, pp. 420-428

[3] LIU, L., LI W., CHEN, X. (2023). Exploration and Realization about Teaching Experimental of CNC Machine Tool Based on Virtual Simulation Technology. In: *Manufacturing Technology*, Vol. 23, No. 4, pp. 485-494

[4] YIN, S., ZHOU, H., JU, X., LI, Z. (2022). Vision-based measurement for decoupling identification of geomeric errors of rotating axes for five-axis platform. In: *Meas Sci Technol*, Vol.33, pp.045007. ISSN 0957-0233

[5] LI, H., ZHANG, P., DENG, M., et al. (2020). Volumetric error measurement and compensation of three-axis machine tools based on laser bidirectional sequential step diagonal measuring method. In: *Meas Sci Technol*, Vol.31, pp.055201. ISSN 0957-0233

[6] LASEMI, A., XUE, D., GU, P. (2016). Accurate identification and compensation of geometric errors of 5-axis CNC machine tools using double ball bar. In: *Meas Sci Technol*, Vol.27, pp.055004. ISSN 0957-0233

[7] ZHANG, L., CHENG, L., LI, J., KE, Y. (2023). Kinematic modeling and error parameter identification of automated fiber placement machine based on measured data. In: *Proc Inst Mech Eng Part B J Eng Manuf*, Vol.237, pp.588-600. ISSN 0954-4054

[8] XIANG, S., YANG, J., ZHANG, Y. (2014). Using a double ball bar to identify position-independent geometric errors on the rotary axes of five-axis machine tools. In: *Int J Adv Manuf Technol*, Vol.70, pp.2071–2082. ISSN 0268-3768

[9] HONG, C., IBARAKI, S. (2012). Non-contact R-test with laser displacement sensors for error calibration of five-axis machine tools. In: *Precis Eng*, Vol.37, pp.159–171. ISSN 0141-6359

[10] SALAMACHA, D., JOZWIK, J. (2023). Evaluation of Measurement Uncertainty Obtained With a Tool Probe on a CNC Machine Tool. In: *Manufacturing Technology*, Vol. 23, No. 4, pp. 513-524

[11] ZHANG, H., XIANG, S., LIU, C. (2022). Reverse identification of dynamic and static motion errors for five-axis machine based on specimen feature decomposition. In: *ISA Trans*, Vol.134, pp.302–311. ISSN 0019-0578

[12] DENG, M., LI, H., XIANG, S. (2020). Geometric errors identification considering rigid-body motion constraint for rotary axis of multi-axis machine tool using a tracking interferometer. In: *Int J Mach Tools Manuf*, Vol.158, pp.103625. ISSN 0890-6955

[13] IBARAKI, S., YUASA, K., SAITO, N., KOJIMA, N. (2018). A Framework for a Large-Scale Machine Tool With Long Coarse Linear Axes Under Closed-Loop Volumetric Error Compensation. In: *IEEEASME Trans Mechatron*, Vol.23, pp.823–832. ISSN 1083-4435

[14] WANG, J., GUO, J. (2016). Geometric error identification algorithm of numerical control machine tool using a laser tracker. In: *Proc Inst Mech Eng Part B J Eng Manuf*, Vol.230, pp.2004–2015. ISSN 0954-4054

[15] ZHAO, Z., HUANG, N., ZHONG, L. (2023). On-machine measurement of thermal influence of the long-span crossbeam of gantry machine tools using a 3D laser profiler. In: *Precis Eng*, Vol.82, pp.52–61. ISSN 0141-6359

[16] YANG, H., HUANG, X., DING, S. (2018). Identification and compensation of 11 position-independent geometric errors on five-axis machine tools with a tilting head. In: *Int J Adv Manuf. Technol*, Vol.94, pp.533–544. ISSN 0268-3768

[17] MARTINEZ-AGUIRRE, M., GOMEZ, G., BO, P. (2024). Design, motion-planning, and manufacturing of custom-shaped tools for five-axis super abrasive machining of a turbomachinery blade type component. In: *Int J Adv Manuf Technol*, Vol.133, pp.655–669. ISSN 0268-3768